Available on CMS information server

CMS CR -2016/207

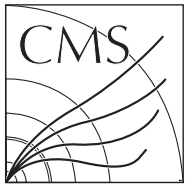

The Compact Muon Solenoid Experiment

Conference Report

Mailing address: CMS CERN, CH-1211 GENEVA 23, Switzerland

01 September 2016 (v5, 15 September 2016)

ttH results from CMS

Eleni Ntomari for the CMS Collaboration

Abstract

First results of the search for the associated top-quark pair and Higgs-boson production ($t\bar{t}H$) in proton-proton collisions with center-of-mass energy $\sqrt{s}$ = 13 TeV are presented. The data correspond to an integrated luminosity of 2.3-2.7 fb^{-1} recorded with the CMS experiment in 2015. The $t\bar{t}H$ process allows a direct measurement of the top-Higgs coupling, which is an important test of the Standard Model (SM), and for searching new physics. Three statistically independent analyses are performed and optimized individually according to different Higgs boson decays, and in each of them, the results are obtained for the signal strength cross section ratio of the measurement to the SM prediction, $\hat{\mu}$=σ/σ_{SM}. The decay to bottom quark-antiquark pair $t\bar{t}H(b\bar{b})$ results in $\hat{\mu}_{obs}^{t\bar{t}H(b\bar{b})} = -2.0^{+1.8}_{-1.8}$, the diphoton decay $t\bar{t}H(\gamma\gamma)$ to $\hat{\mu}_{obs}^{t\bar{t}H(\gamma\gamma)} = 3.8^{+4.5}_{-3.6}$, and the decay to multileptons $t\bar{t}H$(multileptons) results in $\hat{\mu}_{obs}^{t\bar{t}H(multilepton)} = 0.6^{+1.4}_{-1.1}$. A combined result of $\hat{\mu}_{obs}^{t\bar{t}H} = 0.15^{+0.95}_{-0.81}$ is obtained, and is compatible with the SM expectation.

Presented at *LHCP2016 Fourth annual Large Hadron Collider Physics*

PROCEEDINGS OF SCIENCE

Associated top-quark pair and Higgs boson production at CMS with 13 TeV data

Eleni Ntomari on behalf of the CMS Collaboration*
Deutsches Elektronen-Synchrotron (DESY) - Hamburg
E-mail: eleni.ntomari@cern.ch

First results of the search for the associated top-quark pair and Higgs-boson production ($t\bar{t}H$) in proton-proton collisions with center-of-mass energy $\sqrt{s}$ = 13 TeV are presented. The data correspond to an integrated luminosity of 2.3-2.7 fb^{-1} recorded with the CMS experiment[1] in 2015. The $t\bar{t}H$ process allows a direct measurement of the top-Higgs coupling, which is an important test of the Standard Model (SM), and for searching new physics. Three statistically independent analyses are performed and optimized individually according to different Higgs boson decays, and in each of them, the results are obtained for the signal strength cross section ratio of the measurement to the SM prediction, $\hat{\mu}$=σ/σ_{SM}. The decay to bottom quark-antiquark pair $t\bar{t}H(b\bar{b})$ results in $\hat{\mu}^{t\bar{t}H(b\bar{b})}_{obs} = -2.0^{+1.8}_{-1.8}$, the diphoton decay $t\bar{t}H(\gamma\gamma)$ to $\hat{\mu}^{t\bar{t}H(\gamma\gamma)}_{obs} = 3.8^{+4.5}_{-3.6}$, and the decay to multileptons $t\bar{t}H$(multileptons) results in $\hat{\mu}^{t\bar{t}H(multilepton)}_{obs} = 0.6^{+1.4}_{-1.1}$. A combined result of $\hat{\mu}^{t\bar{t}H}_{obs} = 0.15^{+0.95}_{-0.81}$ is obtained, and is compatible with the SM expectation.

Fourth Annual Large Hadron Collider Physics
13-18 June 2016
Lund, Sweden

*Speaker.

1. Introduction

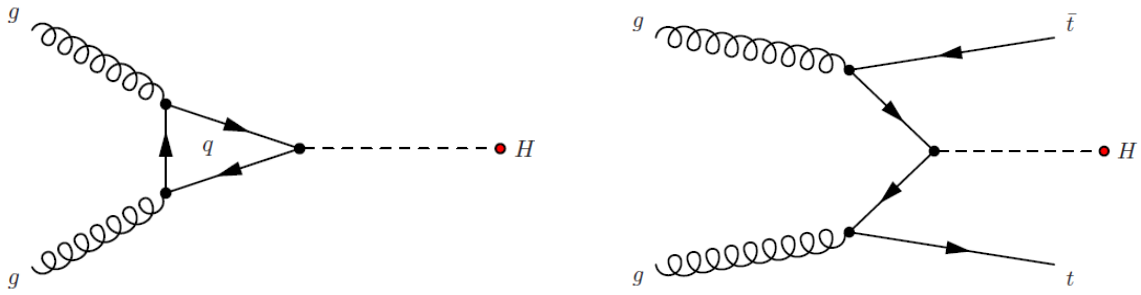

Figure 1: Leading order Feynman diagram of Higgs boson production at LHC. **Left:** gluon-gluon fusion. **Right:** Associated top-quark pair and Higgs boson production.

The LHC Run I data produced at the Large Hadron Collider (LHC) by proton-proton collisions at center-of-mass energies of $\sqrt{s}$ = 7 TeV and 8 TeV, have been exploited by both ATLAS and CMS collaborations, to measure nearly all the accessible properties of the newly-discovered Higgs boson in 2012, with a mass of approximately 125 GeV [2, 3]. After the discovery, the focus lies on measuring its properties in order to find out if the Higgs boson is as predicted by the Standard Model (SM), and irrespective of this, if it reveals any signs of new physics beyond the SM (BSM).

One central aspect to answer these questions is to measure the coupling constants of the boson to the other elementary particles, which depend according to the SM on the mass. The top quark, as the heaviest elementary particle, has the strongest coupling of all. Indirect constraints on the top-quark Higgs boson coupling are available from processes including top-quark loops, for example Higgs boson production through gluon-gluon fusion that is the largest contribution to the total SM Higgs production cross section at the LHC where virtual top quarks dominate this loop-induced process (Fig. 1 (left)) and thus a direct measurement of the coupling is not possible; only indirect constraints using a certain model for interpretation can be deduced. On the other hand, the top-Higgs interaction vertex is directly accessible when the Higgs boson is produced in association with one or more top quarks, since the Higgs boson is too light to decay to top quarks directly. The associated production with a single top quark is suppressed in the SM by interference from couplings of the Higgs boson to the top quark and the W boson; in certain BSM theories this contribution is enhanced and needs to be considered also in corresponding $t\bar{t}H$ interactions. On the other hand, the associated production of a Higgs boson and a top quark-antiquark pair ($t\bar{t}H$ production) is also a direct probe of the top-Higgs coupling, as illustrated in Fig. 1 (right), and offers the best opportunity for measuring its magnitude at the LHC in the SM framework. If observed, it would prove the coupling of the Higgs boson to fermions with weak isospin +1/2 ("up-type") in addition to couplings to τ and b, which carry a weak isospin of -1/2 ("down-type"). Furthermore, several BSM physics models predict a significantly enhanced $t\bar{t}H$ production rate while not modifying the branching fractions of Higgs boson decays by a measurable amount. For example, a number of BSM physics models predict vector-like partners of the top-quark (T) that decay into tH, bW and tZ. The production and decay of TT pairs would lead to final states indistinguishable from those of $t\bar{t}H$ production. In this context, measurement of the $t\bar{t}H$ production cross section has the potential to distinguish the SM Higgs mechanism from alternative mechanisms to generate

fermion masses. Additionally, a comparison of the directly measured top-Higgs coupling with the one inferred by the other cross section measurements can be used to constrain contributions from new physics to the gluon fusion loop. Moreover, once the coupling is obtained, it can be in turn used to search for hidden loop contributions in gluon-gluon fusion.

This report presents the first $t\bar{t}H$ results from CMS at $\sqrt{s}$= 13 TeV using the 2015 dataset. The $t\bar{t}H$ cross section increases by about a factor 4 with the higher center-of-mass energy compared to 8 TeV, while the cross sections of the main backgrounds increase by roughly a factor of 3. The integrated luminosity of the analyzed data correspond to 2.3-2.7 fb^{-1}, which is equivalent to about 50% of the expected number of signal events in 8 TeV data.

The $t\bar{t}H$ decays lead to very complex final states. As the top quark decays almost always to a bottom quark and a W, the decays of the $t\bar{t}$ system are categorized by the decays of the two W bosons: "dileptons" when both W bosons decay leptonically, "lepton+jets" when one of them decays leptonically and the other hadronically, and "hadronic" when both decay hadronically. The "dileptons" channel has the smallest branching ratio, but has the advantage of leading to very clean signatures. On the other hand, the three relevant Higgs boson's decays that can be experimentally identified are categorized as follows. The dominant decay $H(b\bar{b})$ is into bottom quarks, the heaviest particles which can be produced for real, with about 57% probability. H(multileptons) arise from decays to WW^*, ZZ^*, or $\tau\tau$, with at least one Z, W, or τ decaying leptonically. Lastly the decay into photons, $H(\gamma\gamma)$ has a small branching ratio of about 0.2%.

A summary of the results, $\mu_{t\bar{t}H}$=$2.3^{+0.7}_{-0.6}$, with 7 and 8 TeV data (Run I) can be found in Ref. [4] and corresponds to an observed (expected) significance of 4.4σ (2.0σ) over the null hypothesis. The results are obtained from a combined fit of all analysis channels, but the $t\bar{t}$H results are dominated by the measurements in the channels $t\bar{t}H(b\bar{b})$, $t\bar{t}H(\gamma\gamma)$ and $t\bar{t}H$(multileptons) for which dedicated searches were performed.

2. Analysis Strategy and Results

The $t\bar{t}H$ analyses with 13 TeV data are separated by the Higgs boson decays into $t\bar{t}H(b\bar{b})$, $t\bar{t}H(\gamma\gamma)$, $t\bar{t}H$(multileptons) and further subdivided by the $t\bar{t}$ decays. For each of the channels an independent analysis is performed. In each, the corresponding dominant reducible and irreducible background processes are $t\bar{t}$ production in association with other particles. Since the cross sections of these background processes are greater than the signal only, it is crucial to understand them and obtain a good signal-to-background separation. In each analysis, events are classified in two big categories according to the lepton multiplicities and then further subdivided into more categories for better signal-to-background ratios. The analyses are optimized according to the rather low statistics, and several analysis methods are improved compared to the strategies used with 7 and 8 TeV data. All the results are interpreted in the SM using the signal strength.

2.1 $t\bar{t}H(b\bar{b})$

The Higgs boson decay into bottom quark-antiquark pairs ($b\bar{b}$) is attractive as a final state because it features the largest branching fraction of 0.58$\pm$0.02 for a 125 GeV Higgs boson. In addition, both $t\bar{t}H$ production and the decay $H \to b\bar{b}$ only involve third generation quarks, which

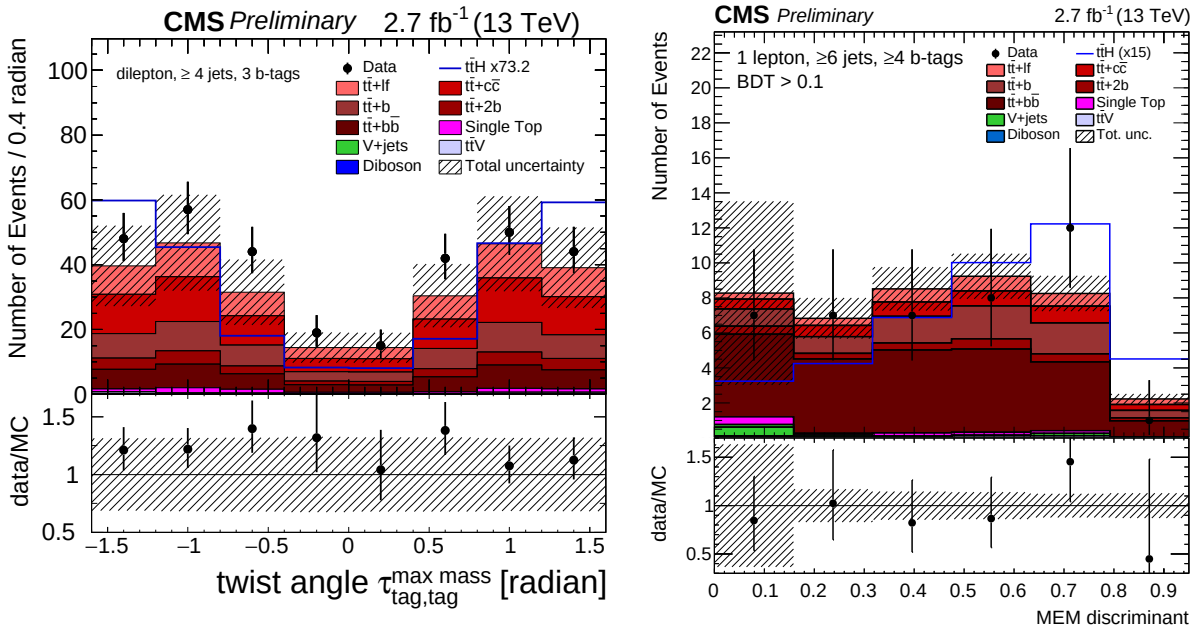

Figure 2: Left: Data-to-simulation comparison of the twist angle between the two b-tagged jets with the maximum mass (BDT input distribution) in the ≥4 jets, 3 b-tags category of the dilepton channel. The expected background contributions (filled histograms) are stacked, and the expected signal distribution (line) for a Higgs-boson mass of m_H= 125 GeV is superimposed. Each contribution is normalized to an integrated luminosity of 2.7 fb^{-1}, and the signal contribution is additionally normalized to the sum of backgrounds for better visibility. The distributions in data (markers) are also shown. **Right:** Final discriminant shape, (MEM with high BDT output), in the category with ≥6 jets, ≥4 b-tags in the lepton+jets channel, before the fit to data. Each contribution is normalized to an integrated luminosity of 2.7 fb^{-1}, and the signal contribution is additionally scaled by a factor of 15 for better visibility.

facilitates the theoretical interpretation of the results. The main challenge comes from the overwhelming background from $t\bar{t}+jets$. Especially the association with two real b-jets is irreducible and theoretically challenging, and thus not yet well understood. Additional challenges come from the limited mass resolution for $H \to b\bar{b}$ and from the presence of many jets with similar kinematics that makes the association to $t\bar{t}$ system or to the Higgs boson ambiguous. The additional jets in $t\bar{t}$+jets, i.e. jets not stemming from the $t\bar{t}$ decay, but from additional radiations, need to be split according to their heavy flavour and treated as independent contributions. The separation is motivated by the fact that different sub-samples originate from different physics processes and have different systematic uncertainties. Thus, the simulated $t\bar{t}$+jets sample is segmented based on the method used in Ref. [5], using the jet clustering to define the jet flavour by injecting hadrons containing b or c quarks with momenta scaled to negligible values into the list of stable particles. The process $t\bar{t}+b\bar{b}$ comprises two or more additional b-jets, like for example jets containing b hadrons, while the label $t\bar{t}+b$ refers to the processes with presence of one additional b-jet containing exactly one b hadron. In principle, these two processes are the same, but in the latter the jets are outside the detector acceptance. On the other hand, the $t\bar{t}+2b$ process has one additional b-jet which contains at least two b hadrons and occurs mainly due to collinear gluon splitting and is theoretically and

experimentally different from the previous.

The main strategy is to constrain the backgrounds and obtain a good signal separation. This is done by forming many orthogonal categories. The two main categories are defined according to the lepton multiplicity of the $t\bar{t}$ system: "lepton+jets" with exactly one lepton and "dilepton" with exactly two opposite sign leptons. The requirements on the leptons suppress the QCD multijet background and are used for triggering. The "lepton+jets" channel has the advantage of high statistics, while the "dilepton" channel profits from minimal non $t\bar{t}$ backgrounds and minimal jet combinatorics.

Signal $t\bar{t}H$ events are generally characterized by having more jets and more b-tags than the background processes. Thus, in order to improve the sensitivity of the analysis, events are then divided into subcategories based on the number of jets and b-tags (jet, b-tag), and the presence of boosted jets from hadronic decays of top quarks or $H \to b\bar{b}$ decays with large transverse momenta; the "boosted" subcategory is new with respect to Run I analysis. For the "lepton+jets" category, the events are separated into eight subcategories: ($\geq$6, 2), (4, 3), (5, 3), ($\geq$6, 3), (4, 4), (5, $\geq$4), ($\geq$6, $\geq$4) and "boosted" and for the "dilepton" category in five subcategories: (3, 2), ($\geq$4, 2), (3, 3), ($\geq$4, 3) and (4, 4). The background-like subcategories with low jet and low b-tag multiplicity constrain the different backgrounds, while the signal-like subcategories following the topology of $t\bar{t}H(b\bar{b})$ have the highest signal-over-background ratios.

Boosted decision trees (BDTs) with different variables and a matrix element method (MEM) are used to achieve the optimal signal separation, in each of the 13 orthogonal subcategories. BDTs are used as the final discovery in the dilepton subcategories and in the "lepton+jets" with exactly 2 jets. An example of a BDT input distribution in a signal-like dilepton subcategory is shown in Fig.2 (left), that confirms that this variable has a good separation power between signal and backgrounds. In the "lepton+jets" subcategories with exactly 3 b-tags as well as in the boosted subcategory, the MEM is used as input in BDTs, while in the subcategories with at least 4 b-tags, where the MEM deploys its full strength, a two dimensional analysis of the two discriminators is performed. An example of this two dimensional analysis can be seen in Fig.2 (right), where MEM is considered as final discriminant, for the ($\geq$6, $\geq$4) "lepton+jets" events with a BDT value greater than 0.1.

Table 1: Asymptotic 95% CL upper limits on the signal strength parameter and the best fit of the signal strength parameter, with 2.7 fb^{-1} 13 TeV (2015) data.

Category	Observed UL	Expected UL $\pm1\sigma$	μ best fit $\pm1\sigma$
opposite-sign dileptons	5.2	$7.7^{+3.6}_{-2.3}$	$-4.7^{+3.7}_{-3.8}$
lepton+jets	4.0	$4.1^{+1.8}_{-1.2}$	$-0.4^{+2.1}_{-2.1}$
combined	2.6	$3.6^{+1.6}_{-1.1}$	$-2.0^{+1.8}_{-1.8}$

Results are obtained from a simultaneous binned maximum-likelihood fit to data in all subcategories. The integrated luminosity of the analyzed data corresponds to 2.7 fb^{-1}. In the "dilepton" category, the signal strength is $\hat{\mu}^{t\bar{t}H(b\bar{b})}_{obs} = -4.7^{+3.7}_{-3.8}$, while in the "lepton+jets" category it is $\hat{\mu}^{t\bar{t}H(b\bar{b})}_{obs} = -0.4 \pm 2.1$. The combined best-fit value of the signal strength is $\hat{\mu}^{t\bar{t}H(b\bar{b})}_{obs} = -2.0 \pm 1.8$ that is 1.7σ below the SM expectation and thus compatible with the no signal assumption [6]. The cor-

responding median expected and observed 95% CL upper limits as well as the signal strength best fit, can be found in Table 1. Since this analysis is systematics dominated, more precise results can be achieved with improvements in theory and modeling as well as with increase of statistics, since it will help to constrain several uncertainties and to understand the backgrounds better.

2.2 $t\bar{t}H(\gamma\gamma)$

Despite the small branching ratio predicted by the SM ($\sim 0.2\%$), the $H \to \gamma\gamma$ decay channel provides a clean final state with an invariant mass peak that can be reconstructed with great precision due to the excellent photon identification and energy resolution.

The analysis is an integral part of the $H \to \gamma\gamma$ analysis [7], where events are categorized according to production mode (Vector Boson Fusion, VBF, and in association with top quarks, $t\bar{t}H$). Those produced via $t\bar{t}H$ are accompanied by two b-quarks and two W bosons, and may be accompanied by charged leptons or additional jets. The analysis is performed with 2.7 fb^{-1} of data preselected with diphoton triggers.

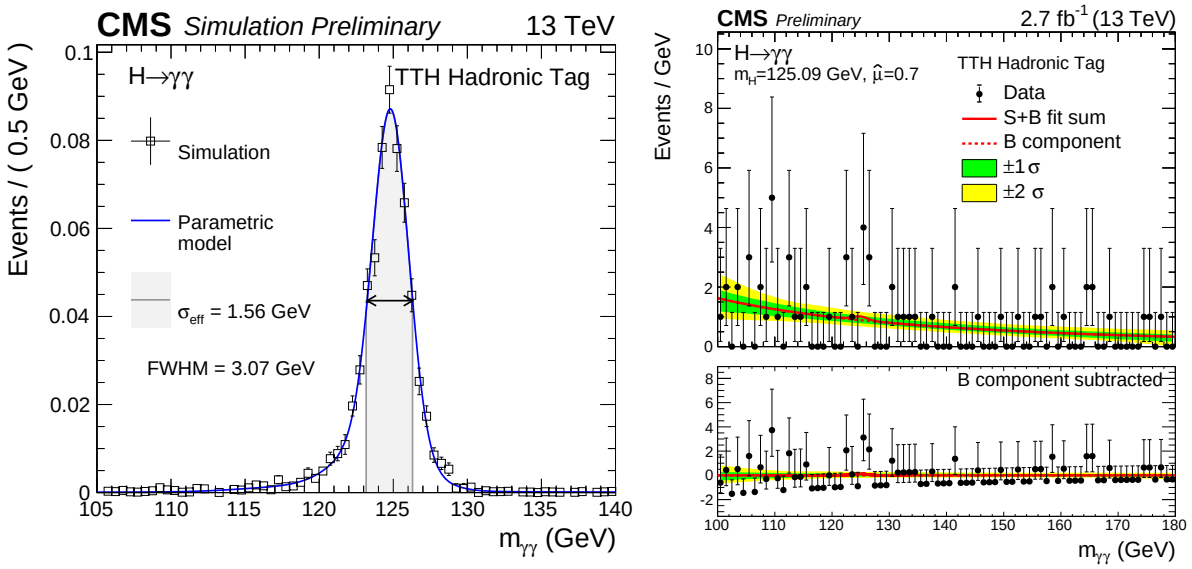

Figure 3: Left: Parametrized signal shape for the "hadronic" category for Higgs boson signal simulated with m_H = 125 GeV. The black points represent weighted simulation events and the blue line is the corresponding parametric model. The σ_{eff} value (half the width of the narrowest interval containing 68.3% of the invariant mass distribution), FWHM, and the corresponding interval, are also shown. **Right:** Diphoton mass spectrum for the "hadronic" category. Data points (black) and S+B model fit (red) are shown. The 1σ (green) and 2σ bands (yellow) include the uncertainties of the fit. The Higgs boson mass is fixed to m_H = 125.09 GeV. The bottom plot shows the residuals after background subtraction.

The main backgrounds stem from the irreducible $t\bar{t} + \gamma\gamma$ and the reducible $t\bar{t} + \gamma$+jet and the $t\bar{t}$+jets where the jets are mis-identified as isolated photons. The main challenges here are the suppression of the mis-identified (fake) photons and corresponding backgrounds and to obtain an excellent diphoton mass resolution. This requires a good photon reconstruction and energy calibration, but also association to the correct primary vertex in the pileup environment. Events are selected with leptons (at least one) from leptonic or semi-leptonic top decays, forming the "lep-

tonic" category, and jets from hadronic top decays, forming the "hadronic" category (no leptons at all). Moreover, at least two jets and at least one b-tag are required in the "leptonic" category, and at least five jets with at least one marked as b-tag, in the "hadronic" category. Different information is combined via a BDT, which is used for photon identification. It is then subsequently used to classify diphoton events via another BDT for signal-like kinematic characteristics, events with good diphoton mass resolution and photon-like values from the photon identification BDT, while avoiding any dependence on the mass itself. This diphoton BDT classifier is used to further select events, requiring values above 0.088 and 0.246 in the "leptonic" and "hadronic" categories respectively.

The event interpretation including signal and background models is identical with the $H \to \gamma\gamma$ analysis, searching for a diphoton mass resonance assuming a non-resonant background. The signal is described with an analytic function, whose parameters are determined by fitting the simulated events in each category and for each of the simulated Higgs boson mass points. For each scenario, the $m_{\gamma\gamma}$ distributions are fitted using a sum of at most five Gaussians. The model is constructed by interpolating with a spline each parameter between individual mass points. For the background, smooth fit functions taking several functional forms are used, where a large set of function families is considered and treated as discrete parameter in a likelihood fit. The fit model is validated in control regions obtained by inverting the photon identification and loosening the event selection.

Fig.3 (left) shows the signal model at 125 GeV Higgs boson mass scenario for the "hadronic category", while the data and the signal plus background model fit (for the "hadronic" category as well) is shown in Fig.3 (right). The 1 σ (green) and 2 σ (yellow) uncertainty bands are shown for the background component of the fit and include the uncertainty in the fitted parameters.

In the dominant "hadronic" category, a small excess of events appears around the mass of the Higgs, while in the more clear "leptonic", only three events pass the event selection criteria, and non of them are observed in this Higgs mass region. The observed signal strength for the combination of the two categories is $\hat{\mu}_{obs}^{t\bar{t}H(\gamma\gamma)} = 3.8^{+4.5}_{-3.6}$, estimated for $m_H = 125.09$ GeV, and is in agreement with the SM within the large uncertainties. The results are statistically limited and thus better precision is expected with increase of statistics.

2.3 $t\bar{t}H$(multileptons)

A third analysis, complementary to $t\bar{t}H(b\bar{b})$ and $t\bar{t}H(\gamma\gamma)$, targets leptonic final states from Higgs boson decays to WW^*, ZZ^*, or $\tau\tau$, with at least one Z, W, or τ decaying leptonically [8]. Despite the small branching ratio, the presence of one or two additional leptons from top quark decays, leads to clean experimental signatures: two same-sign leptons or at least three leptons (electrons or muons), plus b-tagged jets. Since it has the smallest irreducible backgrounds from $t\bar{t}$ associated with vector bosons, $t\bar{t}W$ and $t\bar{t}Z$, the focus lies on understanding the complex reducible background $t\bar{t} + jets$ with fake leptons. The irreducible backgrounds are taken directly from simulation, while the reducible is estimated with data-driven methods.

The general strategy lies on identification, with high efficiency, of prompt leptons and separation from non-prompt and charge mis-identified leptons. The yield of events where one of the selected leptons does not originate from the decay of a W, Z or H boson, is estimated from data using a fake-rate method and the fake rate is estimated from QCD multijet and Z+jets events. The

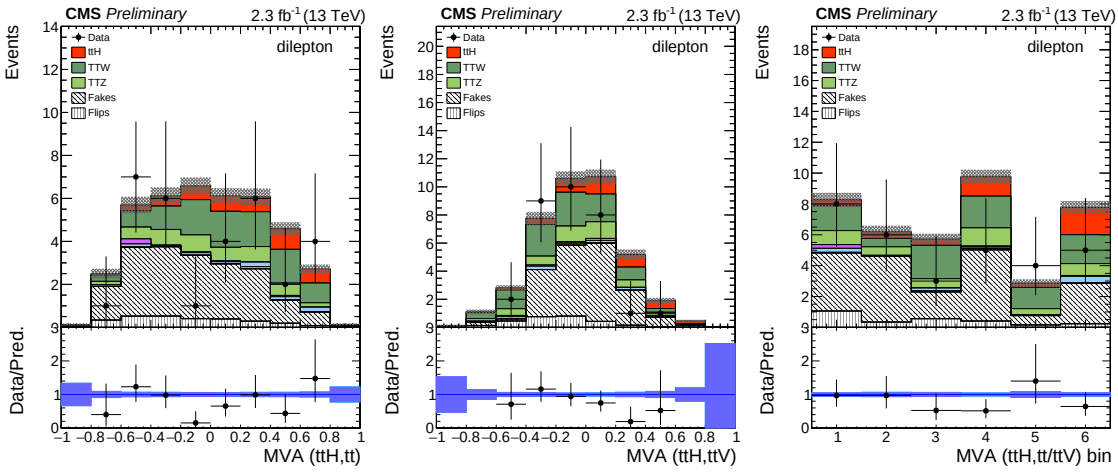

Figure 4: Distributions of the BDT kinematic discriminants and result of their combination in the bins used for signal extraction, for the two same-sign lepton selection inclusive in lepton flavor. Pre-fit distributions are shown. Uncertainties are statistical only.

modelling of the non-prompt lepton backgrounds is aquired from control regions relaxing the lepton selection requirements applied on the BDT used for lepton identification. Afterwards a weight is applied which is a function of the mis-identification probability of the leptons. For electrons also charge mis-reconstruction needs to be considered and is estimated from the dilepton mass spectrum in events selected with same and opposite charge electrons in a sample of electrons from Z decays.

The dataset used for this analysis corresponds to an integrated luminosity of 2.3 fb^{-1}. The events are selected by requiring the presence of either one, two, or three leptons (electrons or muons) at trigger level and are split in two main categories: the "dilepton" that requires exactly 2 same-sign leptons and the "trilepton" that requires at least 3 leptons. The $t\bar{t}$ signature is enhanced by requiring at least 4 and at least 2 jets in the "dilepton" and "trilepton" categories respectively. The analysis strategy is optimized for each category, but to enhance the sensitivity, the events are further sub-categorized according to different background compositions based on lepton charge, the presence of hadronically-decaying τ leptons, the lepton flavour and the presence of at least 2 b-tags. In order to further improve the sensitivity of the analysis, topological and kinematic differences between $t\bar{t}H$ signal and background events are exploited by means of two BDTs, aimed at discriminating the signal from the $t\bar{t}$ and $t\bar{t}V$ processes respectively. The BDTs are trained separately for the two categories and use different sets of input variables for the training against the $t\bar{t}$ and the $t\bar{t}V$ processes. The output of the BDT discriminators is used simultaneously to divide each category in bins of different Signal/Background. The signal extraction is performed by fitting its normalization from the distribution of events among these bins. Figure 4 shows the distributions of the BDT outputs for selected events in data and simulation in the "dilepton" category.

The event yields are compared with the expectation from the background processes and a 125 GeV SM Higgs boson. The best fit of the signal strength parameter in the dominant "dilepton" category and in the "trilepton" are compatible with each other at the level of 1.8σ and their values are $\hat{\mu}_{obs}^{t\bar{t}H(multileptons)} = -0.5^{+1.0}_{-0.7}$ and $\hat{\mu}_{obs}^{t\bar{t}H(multileptons)} = 5.8^{+3.3}_{-2.7}$ respectively (Table 2). A combined best fit of all sub-categories gives a value of $\hat{\mu}_{obs}^{t\bar{t}H(multileptons)} = 0.6^{+1.4}_{-1.1}$ which is in agreement with the

Table 2: Asymptotic 95% CL upper limits on the signal strength parameter and the best fit of the signal strength parameter.

Category	Observed UL	Expected UL $\pm1\sigma$	μ best fit $\pm1\sigma$
same-sign dileptons	2.1	$2.7^{+1.4}_{-0.9}$	$-0.5^{+1.0}_{-0.7}$
trileptons	11.7	$5.4^{+2.9}_{-1.8}$	$5.8^{+3.3}_{-2.7}$
combined	3.3	$2.6^{+1.3}_{-0.8}$	$0.6^{+1.1}_{-1.4}$

SM. Checking the asymptotic 95% CL upper limits on the signal strength parameter (Table 2), we observe slight deficit in the dilepton channel and a small excess in the trilepton. Nevertheless overall there is no significant excess.

3. Combination

Combining the three statistically independent analysis channels described above, assuming a Higgs boson mass of $m_H = 125$ GeV, and correlating the common systematic uncertainties, a signal strength of $\hat{\mu}^{t\bar{t}H}_{obs} = 0.15^{+0.95}_{-0.81}$ is obtained [9], in agreement with the SM expectation ($\hat{\mu}^{t\bar{t}H}_{SM} = 1.00^{+0.96}_{-0.85}$), as can be seen in Fig. 5 (left). The asymptotic 95% CL upper limits on the signal strength parameter for each channel separately and for the combination of them, that corresponds to an observed (expected) value of 2.1 (1.9), are shown in Fig. 5 (right). The green (yellow) bands represent the 1 σ (2 σ) uncertainty bands.

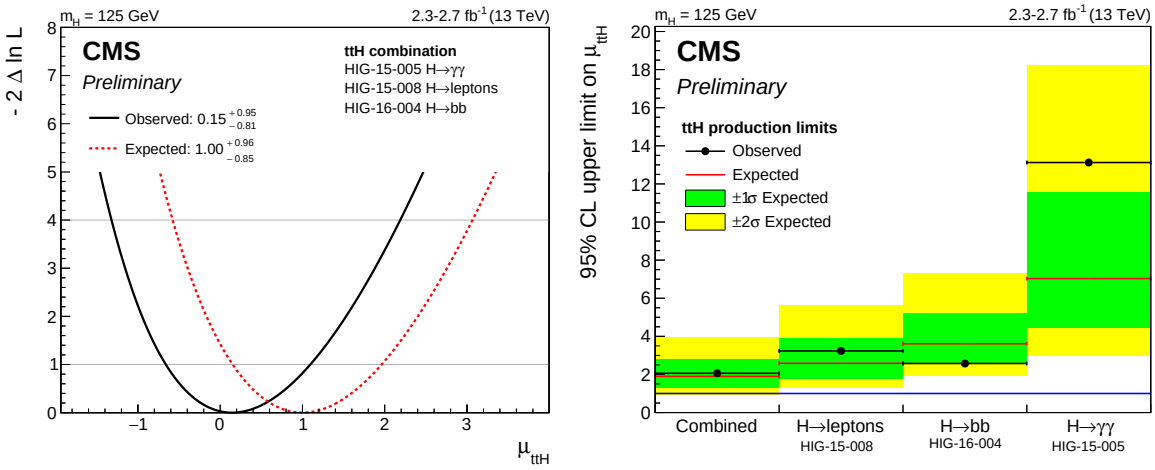

Figure 5: Left: Combined signal strength measurement of the $t\bar{t}H$ production process, via the decays of the Higgs boson to $\gamma\gamma$, $b\bar{b}$ and multileptons. **Right:** 95% confidence level upper limits on the rate of the $t\bar{t}H$ production relative to the standard model expectation, for each channel separately as well as for the combination of them.

4. Conclusions

First results of SM $t\bar{t}H$ production searches, using pp collision data collected by the CMS experiment in 2015 at center-of-mass energy of $\sqrt{s}$ = 13 TeV, has been presented. Independent analyses are performed according to different Higgs decays in $t\bar{t}H(b\bar{b})$, $t\bar{t}H(\gamma\gamma)$ and $t\bar{t}H$(multileptons), each of them using a separate analysis strategy. In $t\bar{t}H(b\bar{b})$ the observed signal strength with a value of $\hat{\mu}_{obs}^{t\bar{t}H(b\bar{b})} = -2.0^{+1.8}_{-1.8}$, is 1.7σ below the SM expectation. In this analysis, as well as in the $t\bar{t}H$(multileptons), multivariate discriminants are used, in order to achieve good signal-to-background separation. In $t\bar{t}H$(multileptons), the observed signal strength is $\hat{\mu}_{obs}^{t\bar{t}H(multilepton)} = 0.6^{+1.4}_{-1.1}$, and within the uncertainties it is in agreement with the SM. Similarly, agreement with the SM is observed in $t\bar{t}H(\gamma\gamma)$, where the signal is extracted from a fit to the invariant diphoton mass distribution and the signal strength is $\hat{\mu}_{obs}^{t\bar{t}H(\gamma\gamma)} = 3.8^{+4.5}_{-3.6}$. Combination of these three analyses, results to a signal strength of $\hat{\mu}_{obs}^{t\bar{t}H} = 0.15^{+0.95}_{-0.81}$, that is also in agreement with the SM.

This compares to a best-fit of $\hat{\mu}_{obs}^{t\bar{t}H} = 2.8^{+1.0}_{-0.9}$ in Run I, that was derived with double of statistics. Nevertheless, the sensitivity is similar mainly due to the improved analysis techniques used in Run II. The expected luminosity with full 2016 data is expected to be in the order of 25 fb^{-1} and thus many more results are about to come, hopefully leading to the observation of the $t\bar{t}H$ production mode and eventually to the measurement of the top-Higgs coupling.

References

[1] CMS Collaboration, "*The CMS experiment at the CERN LHC*", JINST 3 S08004 (2008).

[2] ATLAS Collaboration, "*Observation of a new particle in the search for the Standard Model Higgs boson with the ATLAS detector at the LHC*", Phys. Lett. B 716, 1 (2012).

[3] CMS Collaboration, "*Observation of a new boson at a mass of 125 GeV with the CMS experiment at the LHC*", Phys. Lett. B 716, 30 (2012).

[4] ATLAS and CMS Collaborations, "*Measurements of the Higgs boson production and decay rates and constraints on its couplings from a combined ATLAS and CMS analysis of the LHC pp collision data at $\sqrt{s}$ = 7 and 8 TeV*", ATLAS-CONF-2015-044, CMS-PAS-HIG-15-002.

[5] CMS Collaboration, " *Measurement of $t\bar{t}$ production with additional jet activity, including b quark jets, in the dilepton decay channel using pp collisions at $\sqrt{s}$ = 8 TeV*", Eur. Phys. J. C. 76 (2016) 379.

[6] CMS Collaboration, "*Search for $t\bar{t}H$ production in the $H \to b\bar{b}$ decay channel with $\sqrt{s}$ = 13 TeV pp collisions at the CMS experiment*", CMS-PAS-HIG-16-004.

[7] CMS Collaboration, "*First measurements of the Higgs boson production in the diphoton decay channel at $\sqrt{s}$ = 13 TeV*", CMS-PAS-HIG-15-005.

[8] CMS Collaboration, "*Search for $t\bar{t}H$ production in multilepton final states at $\sqrt{s}$ = 13 TeV*", CMS-PAS-HIG-15-008.

[9] CMS Collaboration, ttH Combination public webpage, *https://twiki.cern.ch/twiki/bin/view/CMSPublic/TTHCombMoriond2016*.